Quaternary Science Reviews 302 (2023) 107932

Contents lists available at ScienceDirect

Quaternary Science Reviews

journal homepage: www.elsevier.com/locate/quascirev

New vegetation history reconstructions suggest a biostratigraphic assignment of the lowermost Rodderberg interglacial (Germany) to MIS 11

Patrick Schläfli [a, b, *], Erika Gobet [b], Ines Hogrefe [c], Felix Bittmann [c, d], Fritz Schlunegger [a], Bernd Zolitschka [c], Willy Tinner [b]

[a] Institute of Geological Sciences, University of Bern, Switzerland
[b] Institute of Plant Sciences and Oeschger Centre for Climate Change Research, University of Bern, Switzerland
[c] Institute of Geography, University of Bremen, Germany
[d] Lower Saxony Institute for Historical Coastal Research, Wilhelmshaven, Germany

ARTICLE INFO

Article history:
Received 2 August 2022
Received in revised form
22 November 2022
Accepted 18 December 2022
Available online xxx

Handling Editor: Yan Zhao

Keywords:
Lowermost Rodderberg interglacial
Middle Pleistocene
MIS 11
Pollen analysis
Biostratigraphy
Vegetation dynamics

ABSTRACT

Along with the ongoing climate crisis, research efforts increasingly focus on Pleistocene environmental archives. Interglacial periods are of special interest, as they offer crucial information about natural interactions (i.e. not influenced by human activities) between climate and ecosystems within a climatic setting comparable to the Holocene and/or climate change projections. The sedimentary infill of the Rodderberg crater, 10 km south of the city of Bonn (Germany), records several glacial-interglacial cycles in superposition, which makes it a rare and promising environmental archive. One of the most challenging targets is to establish a robust chronological framework for the Rodderberg sediment sequence. In the present study we reconstruct the vegetation history of the basal and most prominent interglacial sequence, the lowermost Rodderberg interglacial (LRI), and apply the principles of pollen biostratigraphy to estimate the depositional age. At the base of the sequence steppe tundra conditions prevailed during the cryocratic phase before the onset of the interglacial. Rising temperatures caused afforestation of the landscape with boreal forests during the protocratic phase, which subsequently were replaced by temperate forests in the mesocratic phase. The sequence continues under unstable vegetation conditions characterized by temperate forests dominated by *Carpinus* and *Abies* during the oligocratic phase. During the terminal part of the LRI, the telocratic phase, boreal to nemoboreal forests covered the landscape. Due to climatic deterioration these forests collapsed and a steppe tundra evolved again (cryocratic phase). This climate-driven glacial-interglacial cycle is followed by an interstadial with rather closed nemoboreal forest vegetation. Based on the occurrences of characteristic taxa as well as the vegetation assemblages and succession, we refrain from correlating the LRI with any of the warm stages between c. 240 and 180 ka BP, i.e. roughly corresponding to MIS 7. A correlation with the Holsteinian, which was previously physically dated to c. 340–325 ka BP, cannot unambiguously be excluded, however, the absence of *Pterocarya* during the LRI argues against it. Instead, the LRI has striking similarities with the Kärlich interglacial, which has been previously physically dated to c. 400 ka BP, making it chronologically equivalent to MIS 11.

1. Introduction

Ongoing human-induced climate warming is increasingly pressuring natural systems around the globe. To predict future impacts of climate change, it is crucial to understand the complex and often non-linear relations between climate forcing and ecosystem behaviour (Williams et al., 2021). Here, Pleistocene sediment records offer unique possibilities to study environmental dynamics as responses to climate change on various timescales, at various degrees of intensity, and under negligible anthropogenic influences. Among the limiting factors, the discovery of suitable natural archives and the establishment of robust chronologies are

* Corresponding author. Institute of Geological Sciences, University of Bern, Switzerland.
E-mail address: patrick.schlaefli@geo.unibe.ch (P. Schläfli).

https://doi.org/10.1016/j.quascirev.2022.107932

the most challenging to overcome. Despite the availability of various dating techniques appropriate for the Early and Middle Pleistocene (e.g. luminescence, U/Th, isochron burial dating), their applicability is highly specific and the obtained ages are often minimum ages and/or are associated with high uncertainties (Geyh, 2008; Knudsen et al., 2020; Dieleman et al., 2022; Schwenk et al., 2022). Another way to chronologically constrain a sedimentary sequence is offered by biostratigraphy, because vegetational successions and compositions vary among Pleistocene interglacials, resulting in pollen-based interglacial signals with characteristic vegetational fingerprints (Bittmann, 1992; Litt, 2007; Kühl and Gobet, 2010; Stebich et al., 2020; Schläfli et al., 2021).

The Rodderberg Volcanic Complex (RVC; 147 m a.s.l.), situated c. 10 km south of the city of Bonn in Germany (Fig. 1), contains an ideal archive to disclose past environmental changes. In a study documenting the 164 m-long drill core ROD11-1 from the central area of the crater of the RVC, Zolitschka et al. (2014) identified sediments possibly recording three consecutive interglacials for which the authors provided a tentative age assignment (Fig. 2). The lower age boundary is inferred from luminescence dates of tuff and a siltstone xenolith and lies in the range between 300 and 500 thousand years (ka) before present (Paulick et al., 2009; Zöller and Blanchard, 2009). Two luminescence dates from an earlier coring in the central area of the crater (Zöller et al., 2011) are projected onto the sedimentary sequence of ROD11-1 by correlating distinct patterns of the magnetic susceptibility curves of both drill cores. These ages of 107 ± 13 (TL) and 66 ± 13 ka (IRSL) correspond to a depth of 57.5 m in the ROD11-1 core, which is right above the lowest interglacial. Such young ages would imply that the superposed interglacials would correspond to interstadials. However, the ages were interpreted as underestimating the true deposition age, since no fading correction was used and the equivalent doses were almost saturated (Schmidt et al., 2011a, 2011b; Zolitschka et al., 2014). This finding agrees with the biostratigraphic evidence obtained so far. Eight subsamples have been taken within the sediments of all three interglacials for a preliminary study. Their fossil pollen content (Fig. 2) revealed that none of the three interglacial assemblages allows an unambiguous correlation with known pollen records. Nevertheless, a tentative biostratigraphic assignment was attempted (Zolitschka et al., 2014). In fact, a correlation of the lowermost Rodderberg interglacial (LRI) with MIS 5e can be

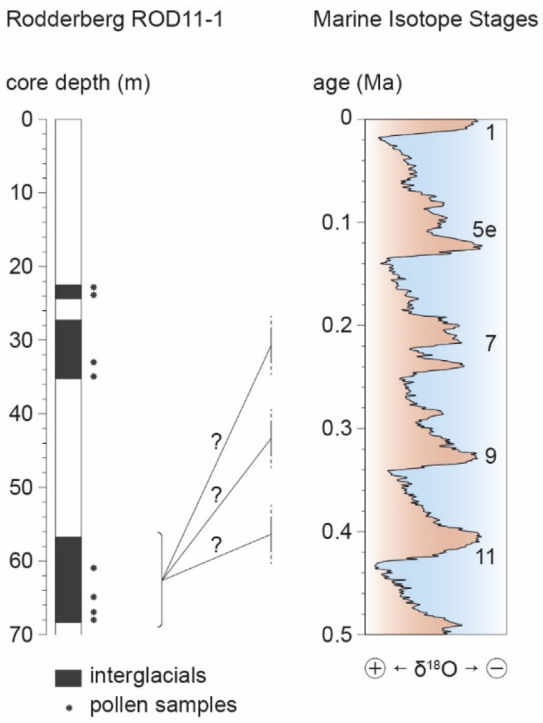

Fig. 2. Possible scenarios for the Rodderberg sediment sequence ROD11-1 within the chronostratigraphic framework of the Marine Isotope Stages (MIS; modified after Lisiecki and Raymo, 2005). Three phases with high total organic carbon (TOC) content (black bars) have been identified during a low-resolution (1-m sampling intervals) study of core-catcher samples by Zolitschka et al. (2014) and preliminary pollen analysis (•) suggest the presence of three consecutive interglacials. In this study, we investigate the palynological content of the lowermost interglacial (LRI) to reconstruct its vegetational history and to estimate its chronological position.

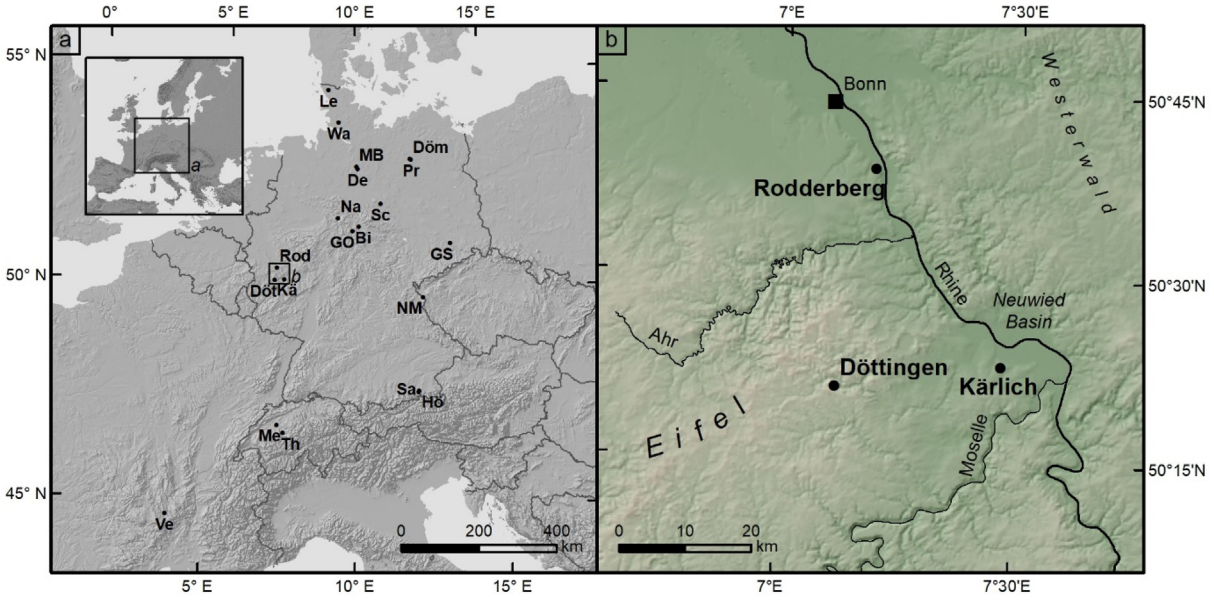

Fig. 1. Site map of Rodderberg. a) European key sites mentioned in the text Bi = Bilshausen, De = Dethlingen, Döm = Dömnitz, Döt = Döttingen, GO = Göttingen/Ottostraße, GS = Gröbern-Schmerz, Hö = Höhenmoos, Kä = Kärlich, Le = Leck, MB = Munster-Breloh, Me = Meikirch, Na = Nachtigall, NM = Neualbenreuth Maar, Pr = Pritzwalk, Rod = Rodderberg, Sa = Samerberg, Sc = Schöningen, Th = Thalgut, Ve = Velay, Wa = Wacken. b) Topographic map of the study area showing the Rodderberg and its two closest possible analogues Döttingen (Diehl and Sirocko, 2007) and Kärlich (Bittmann, 1992).

excluded due to the presence of *Celtis* pollen. Additionally, the pollen assemblages of the four samples taken from the lowermost interglacial showed similarities with the Kärlich interglacial (Bittmann, 1992) and the Holsteinian interglacial from Döttingen (Diehl and Sirocko, 2007), which may fall into MIS 9 or MIS 11 (e.g. Reille et al., 2000; Geyh and Müller, 2005). However, the four pollen samples previously analysed within the LRI did clearly not suffice for a careful biostratigraphic assignment.

The Rodderberg sequence has the potential to be an exceptional environmental archive for Central Europe, since long sequences spanning several glacial-interglacial cycles are rare. An age assignment is crucial for the understanding of the dynamics between climate forcing and environmental dynamics. Therefore, we aim at (1) providing an overview of the vegetation history of the LRI and (2) clarifying the vague chronology of its sedimentary sequence by biostratigraphically assigning the vegetational composition, structure, and succession to previously reconstructed Central and Western European interglacial vegetation dynamics.

2. Materials and methods

2.1. Current climate and vegetation

The current climate in the region is characterized as temperate (Cfb; Kottek et al., 2006) with January and July mean temperatures of 2.5 and 18.9 °C, respectively. The annual mean precipitation of 939 mm is well distributed over the year with April (59 mm) as driest and December (96 mm) as wettest month. All data has been retrieved from the meteorological station Bad Godesberg (68 m a.s.l.; period 1991–2021), c. 5 km NW of Rodderberg.

The current vegetation around Rodderberg is highly influenced by human impact. Isolated patches of protected forests (e.g. Kottenforst and Waldville) grow in an agriculturally-exploited landscape. Much of these forests were reforested since the 1970s on former brown coal mines and are composed of various forest types. Diverse broadleaved (e.g. *Acer platanoides*, *Alnus glutinosa*, *Betula pendula*, *Carpinus betulus*, *Corylus avellana*, *Fagus sylvatica*, *Fraxinus excelsior*, *Prunus padus*, *Quercus robur*, *Sorbus aucuparia, Tilia cordata*) and coniferous (e.g. *Larix decidua*, *Picea abies*, *Pinus sylvestris*) shrubs and trees characterize the forest assemblages (Erdelen, 1984). Old-growth beech (*Fagus sylvatica*) forests in the larger study area (e.g. in the Eifel National Park; Schmiedel et al., 2019) are relicts of the vegetation prior to 20th reforestation activities.

2.2. Lithology

For the present study sedimentary material of the second (ROD11-2) of three parallel cores taken in 2011 at a distance of c. 1 m from each other was chosen. The depths we refer to are in meter composite depth (m) based on high-resolution correlation of the two parallel and overlapping core series ROD11-2 and ROD11-3 (Hogrefe et al., *in prep.*). This procedure is the reason for minor discrepancies in depths compared to Zolitschka et al. (2014), who worked exclusively with core-catcher material from rotary flush-drilling ROD11-1 and not with sediment cores (Fig. 2). We classify the sediment of ROD11-2 between 70.8 and 58.9 m according to Troels-Smith as also reported in e.g. Aaby and Berglund (1986) and Kershaw (1997).

2.3. Palynological analyses

We analysed 82 samples of 0.5 cm^3 between 70.8 and 58.9 m for their fossil pollen and spore content. The sample resolution is generally 20 cm and was increased to 6 or 8 cm between 69 and 67 m. To estimate pollen and spore concentrations, we added *Lycopodium* tablets (Stockmarr, 1971) before physical (sieving with 500 μm mesh) and chemical treatment of the samples (HCl, KOH, HF, acetolysis; Moore et al., 1991). The pollen samples were stained with fuchsine and mounted on microscopic slides in glycerine. Pollen and spore identification follows the keys by Moore et al. (1991) and Beug (2004), the palynological atlas of Reille (1992) and the reference collection of the Institute of Plant Sciences, University of Bern. A transmitted light microscope with 400x or 1000× magnification was used. The distinction between tree and shrub *Betula* is based on Birks (1968) and Clegg et al. (2005). *Fraxinus excelsior*- and *F. americana*-type were distinguished according to Bittmann (1991). We aim at a total terrestrial pollen sum of >500 grains (excl. Cyperaceae) per sample. Percentages were calculated with respect to the total terrestrial pollen sum (= 100%) excluding Cyperaceae. Pollen grains were classified as indeterminable (= 'indet') if characteristic features were not recognizable, e.g. due to fragmentation, immobility, or masking by residuals in the sample.

2.4. Numerical analyses

We use the optimal partitioning with minimum sum-of-squares approach (Birks and Gordon, 1985) and the broken stick criterion (Bennett, 1996) to divide the pollen diagrams into statistically significant local pollen assemblage zones (LPAZ). Additional sub-zones were assigned visually. For the Principal Component Analysis (PCA) the software Canoco 5.10 (ter Braak and Šmilauer, 2018) is applied. Prior to the PCA the pollen percentage data was log transformed. The gradient length (2.1 SD units) of the data set justifies the use of a linear method.

3. Results and interpretations

3.1. Lithology

The lowermost part of the studied core segment consists of laminated (70.9–70.4 m) and partly laminated (70.4–69 m) grey silt layers. Subsequently, the material is characterized by laminated, black gyttja deposits (69–68.1 m), which are interrupted by a 2 cm-thick tephra layer at 68.9 m. From 68.1 m upwards, the sediments gradually become sandier and dark greyish brown in colour. Laminations occur less frequently in this part. A gradual change towards laminated, black gyttja deposits occurs around 67.1 m. Between 66.2 and 62 m the sediments predominantly consist of dark greyish brown sand, which is partly laminated. After a rather sharp change at 62 m the material is characterized as dark, laminated gyttja. Above, the material gets sandier and laminations do not occur anymore. From 61.5 m to the top of the studied section, the sediments are predominantly massively bedded (and thus unlaminated) olive-grey to dark-grey silts (61.4–58.9 m).

3.2. Numerical analysis of pollen data

The zonation of the 82 pollen samples yielded eleven statistically significant local pollen assemblage zones (LPAZ; ROD-1 to ROD-11), eight additional sub-zones were assigned visually. A total terrestrial pollen sum of >500 was achieved in 74 samples. In the samples between 70.8 and 69.3 m (n = 8), in which pollen preservation and/or concentration was particularly bad and/or low, a pollen sum of 100–200 was achieved. This results in an average terrestrial pollen sum of 480 grains per sample.

To summarize the main gradients within the pollen data, we applied a Principal Component Analysis (PCA). The first two axes of which account for 52.6% of the total variance with PCA axis 1 contributing 40.5% and PCA axis 2 12.1%. Thus, they represent the

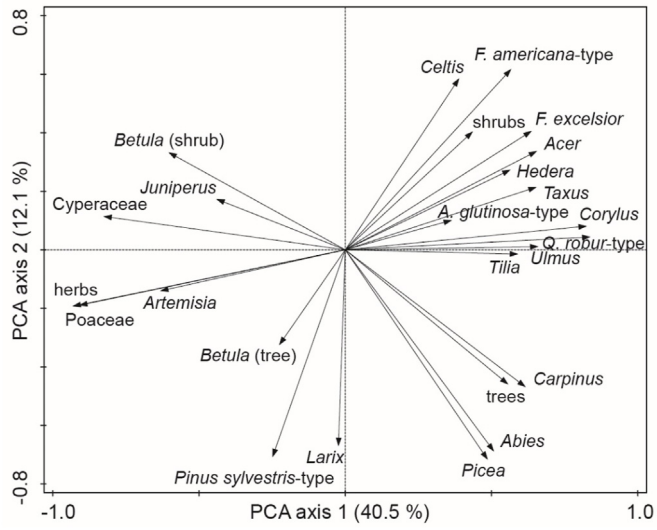

Fig. 3. Species scores (selected taxa) of the principal component analysis (PCA). Axis 1 (axis 2) explains 40.5% (12.1%) of the total variance within the data set. The horizontal and the vertical components of the arrows are proportional to their contribution to the total variance explained along axis 1 and axis 2, respectively. Axis 1 represents a climate driven gradient from open grassland and shrubby (Poaceae, Cyperaceae, *Artemisia*, shrub *Betula*, *Juniperus*) and boreal forest vegetation (tree *Betula*, *Pinus sylvestris*-type) to closed temperate forest vegetation. *F.* = *Fraxinus*; *A.* = *Alnus*; *Q.* = *Quercus*. Sample scores of the PCA are plotted within the main pollen percentage diagram (Fig. 4).

main gradients within the pollen dataset (Fig. 3). Shrub *Betula*, boreal tree taxa such as *Juniperus,* tree *Betula,* and *Pinus sylvestris* as well as herbs (e.g. *Artemisia*, Poaceae) have negative species scores on axis 1. Deciduous temperate tree taxa such as *Quercus robur*-type, *Corylus*, *Fraxinus excelsior*-type, *Ulmus*, *Tilia, Carpinus* as well as evergreen temperate arboreal taxa such as *Hedera*, *Abies,* and *Taxus* have positive scores along axis 1. Boreal *Picea* is also within this rather mesophilous group. Most positive species scores along axis 2 are reached by *Fraxinus americana*-type and *Celtis*, most negative by *Picea*, *Pinus sylvestris*-type, *Abies*, and *Larix*. The latter include the conifers, among them trees which can grow very tall (e.g. *Abies* and *Picea* with >50–60 m), while positive species scores are associated to lower growing taxa, e.g. shrubs with <10 m. Most positive sample scores along axis 1 are reached in descending order by samples from ROD-6, ROD-4, ROD-5, and ROD-7, for the latter especially samples of the lower part of the zone (Fig. 4). Most negative sample scores along axis 1 are reached by samples of zones ROD-1 and ROD-9.

3.3. Pollen stratigraphy and vegetation history of the LRI

3.3.1. Cryocratic (glacial) vegetation (ROD-1; 70.8–69.3 m)

Pollen preservation and concentration are generally poor in ROD-1, resulting in high amounts of indeterminable pollen grains and lower-than-average terrestrial pollen sums. The assemblages are dominated by pollen of herbaceous taxa, mainly Poaceae, *Artemisia*, and Cyperaceae, but also Chenopodiaceae, Caryophyllaceae, and Brassicaceae. Percentages and concentrations of *Betula* (tree and shrub) pollen increase towards the end of the zone, together with decreasing percentages and slightly increasing concentrations of *Pinus sylvestris*-type pollen. Within the whole sequence, percentages of *Alnus glutinosa*-type are highest in the first half of this zone. Pollen from other woody taxa such as *Salix*, *Picea*, *Corylus*, and Ericaceae is continuously present. Single grains of *Carpinus*, *Quercus robur*-type, *Ulmus*, and *Pterocarya* are found in this zone.

Based on these results, we infer the presence of steppe tundra vegetation with scattered boreal forest stands consisting of *Pinus sylvestris* and *Betula* trees. The abundances of both woody taxa increased towards the end of this zone, as inferred from increasing pollen percentages and concentrations. *Alnus incana* (*Alnus glutinosa*-type pollen) was probably growing around the crater lake where the soil was water saturated. We assume the presence of *Alnus incana* because it is better adapted to colder conditions than *A. glutinosa* (Houston Durrant et al., 2016), with a current northern distribution limit at the forest border in Scandinavia and Russia (Hytteborn et al., 2005). Likewise, shrubs such as *Salix, Juniperus, Corylus avellana*, and *Picea* trees were possibly already present in the catchment. Sporadic occurrences of temperate taxa such as *Carpinus*, *Quercus*, *Ulmus*, and *Pterocarya* may indicate that these pollen grains were reworked from older deposits, perhaps from upper crater banks. This interpretation is supported by the bad preservation of these grains and their low concentrations. Less likely, long-distance transport from more southerly populations may explain the occurrences of pollen grains of these temperate taxa.

3.3.2. Protocratic (pre-temperate) interglacial vegetation (ROD-2; 69.3–69 m)

Pollen preservation in ROD-2 is slightly better compared to ROD-1, resulting in less indeterminable grains and higher terrestrial pollen sums (>500). Pollen concentrations are also generally higher than in ROD-1 (Fig. 5). Percentages of arboreal pollen (AP) increase from c. 60% at the beginning to c. 90% towards the end of the zone (Figs. 4 and 6). The remaining herbaceous pollen types are mainly *Artemisia*, Poaceae, *Thalictrum*, and Apiaceae. Pollen of tree and shrub *Betula* dominates the assemblage. Similar to the previous zone, the percentages of *Pinus sylvestris*-type continue to decrease in ROD-2. *Salix* pollen declines compared to ROD-1. *Celtis* and *Quercus robur*-type pollen has continuous abundances, and single grains of *Hedera* were found.

These results suggest that climate warming during the protocratic stage of the interglacial may have led to the establishment of boreal forests dominated by *Betula* trees. Shrub *Betula* (possibly *B. nana*) occupied open landscapes (peak in percentages and concentrations) at the expense of herbaceous tundra vegetation. *Alnus* (probably still *A. incana*, possibly also *A. glutinosa*) as well as tree and shrub species of *Salix* were present in the area. Temperate deciduous shrubs and trees like *Corylus*, *Ulmus* (possibly *U. glabra*), *Quercus*, and *Celtis* were present in the study area at the end of zone ROD-2.

3.3.3. Mesocratic (early-temperate) interglacial vegetation (ROD-3 to ROD-6; 69–68.3 m)

In ROD-3 the amount of indeterminable pollen grains further decreases due to a better preservation compared to ROD-2. Percentages of tree pollen reach >90% with main contributions by *Pinus sylvestris*-type and tree *Betula* pollen, both also showing higher pollen concentrations compared to the previous zone. Pollen of *Salix* shows highest concentrations within the whole sequence, while percentages and concentrations of shrub *Betula* decline. *Ulmus*, *Fraxinus excelsior*-, and *F. americana*-type reach their empirical pollen limit and concentrations of *Alnus glutinosa*-type pollen start to increase.

ROD-4 is characterized by pollen preservations comparable to ROD-3. Percentages of arboreal pollen (AP) stay >95% and those of *Corylus* strongly increase in this zone (to c. 60%), mostly at the expense of *Pinus sylvestris*-type and tree *Betula* pollen abundances. Percentages and concentrations of *Quercus robur*-type massively increase, while *Fraxinus excelsior*-type and *Ulmus* show a slight

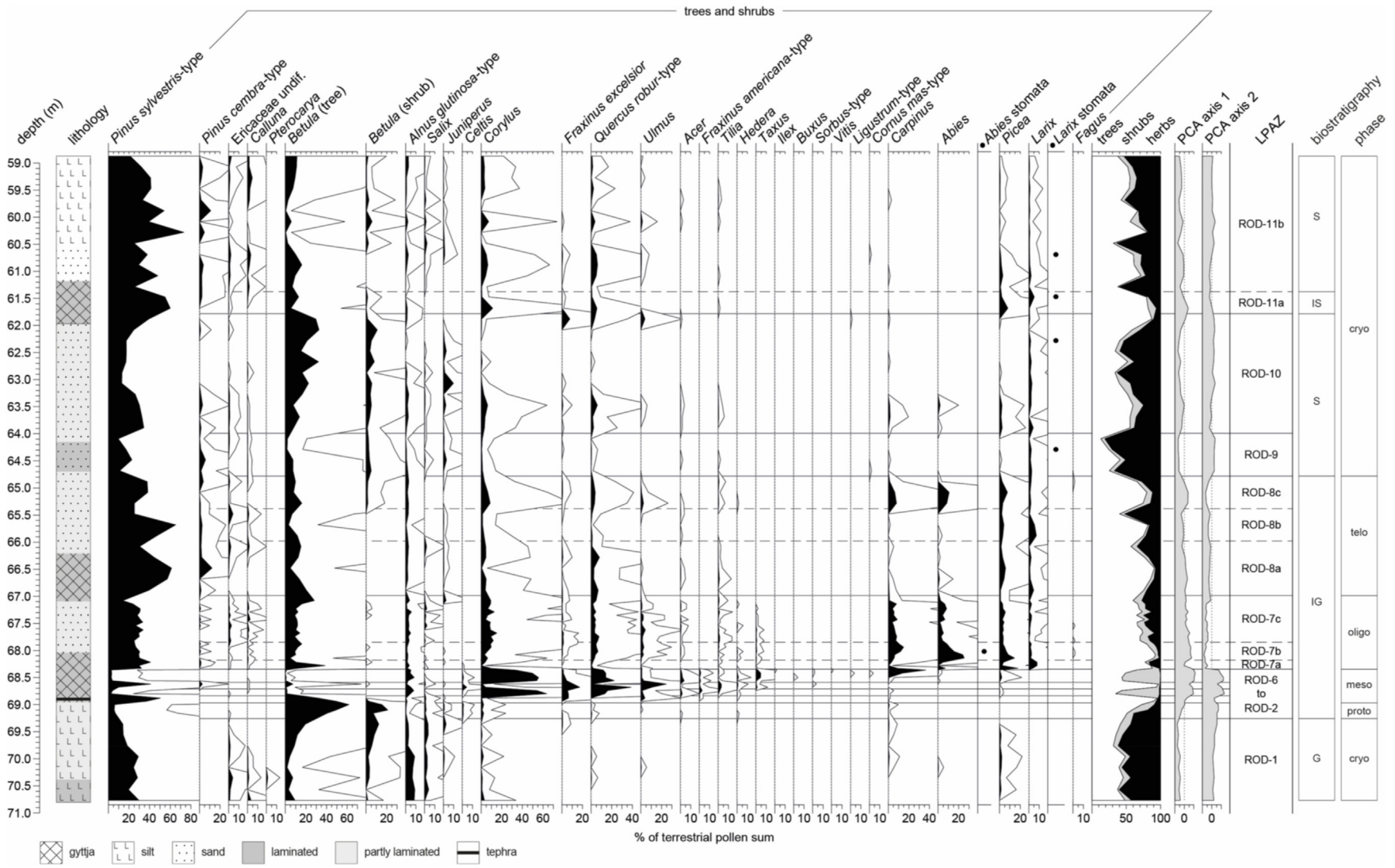

Fig. 4. Pollen percentage diagram (selected taxa). Black lines represent 10x exaggeration. PCA = sample scores of the Principal Component Analysis. Stomata findings are marked as black dots. Statistically significant local pollen assemblage zones (LPAZ) are delimited with continuous lines, visually assigned sub-zones are represented by dashed lines. The biostratigraphical assignments read G = glacial, IG = interglacial, S = stadial, IS = interstadial. Phases according to the glacial-interglacial cycle (see Birks and Tinner, 2016) are cryo = cryocratic, proto = protocratic, meso = mesocratic, oligo = oligocratic, telo = telocratic. Parts of the interglacial section are shown in more detail in Fig. 6.

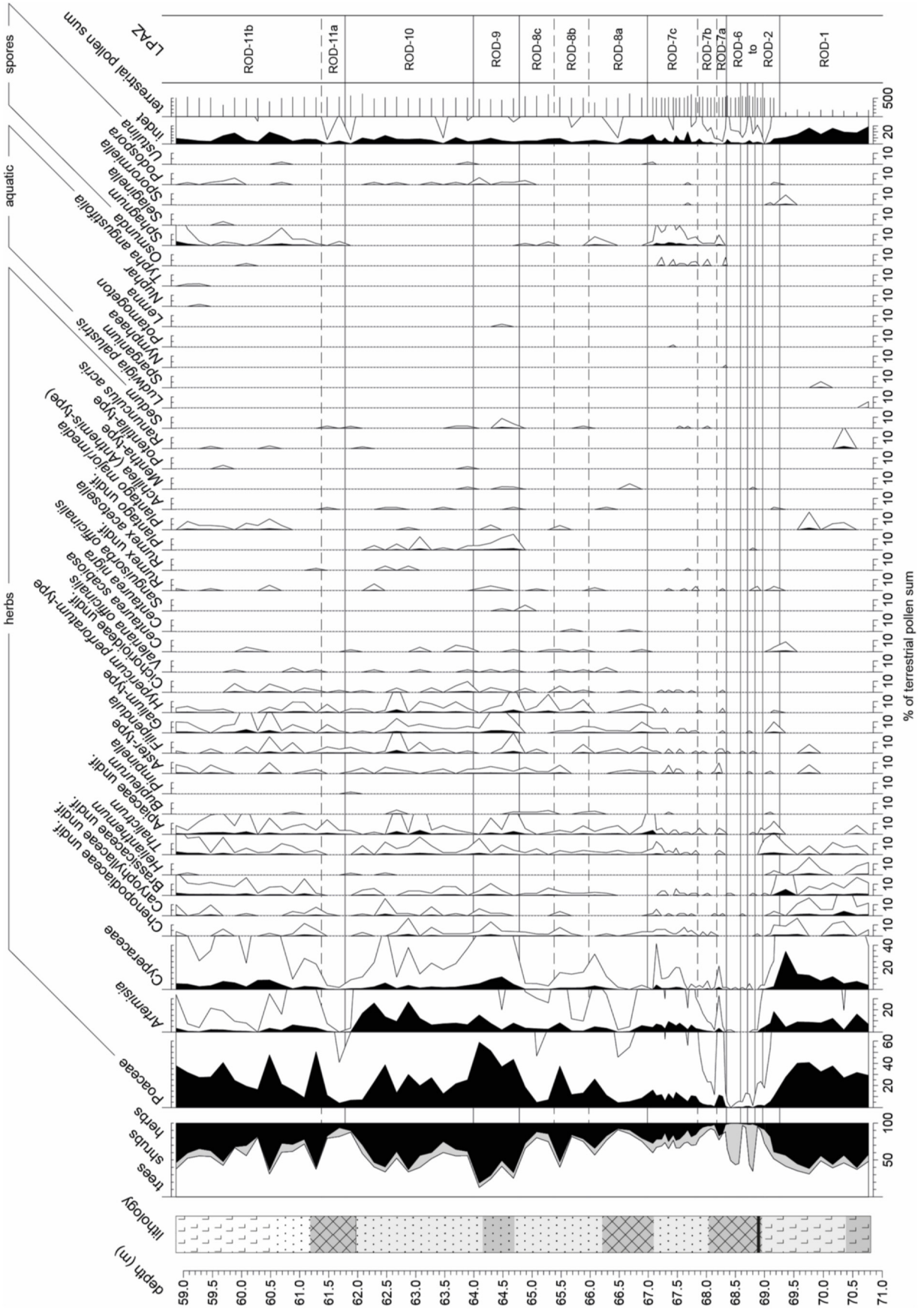

Fig. 4. (*continued*).

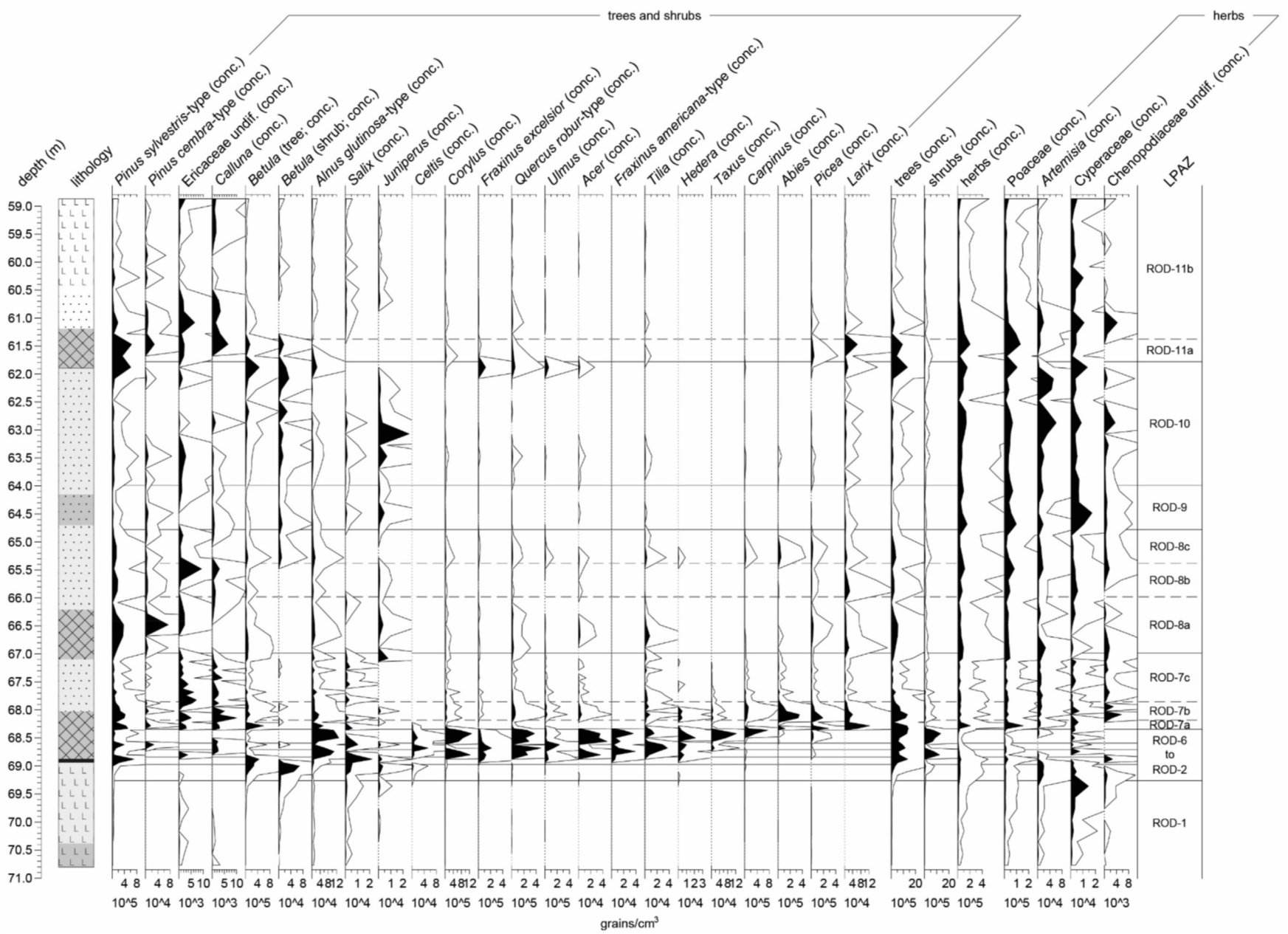

Fig. 5. Pollen concentration diagram (selected taxa). Black lines represent 10x exaggeration (lithological key: see Fig. 4). Data is shown on non-uniform scales.

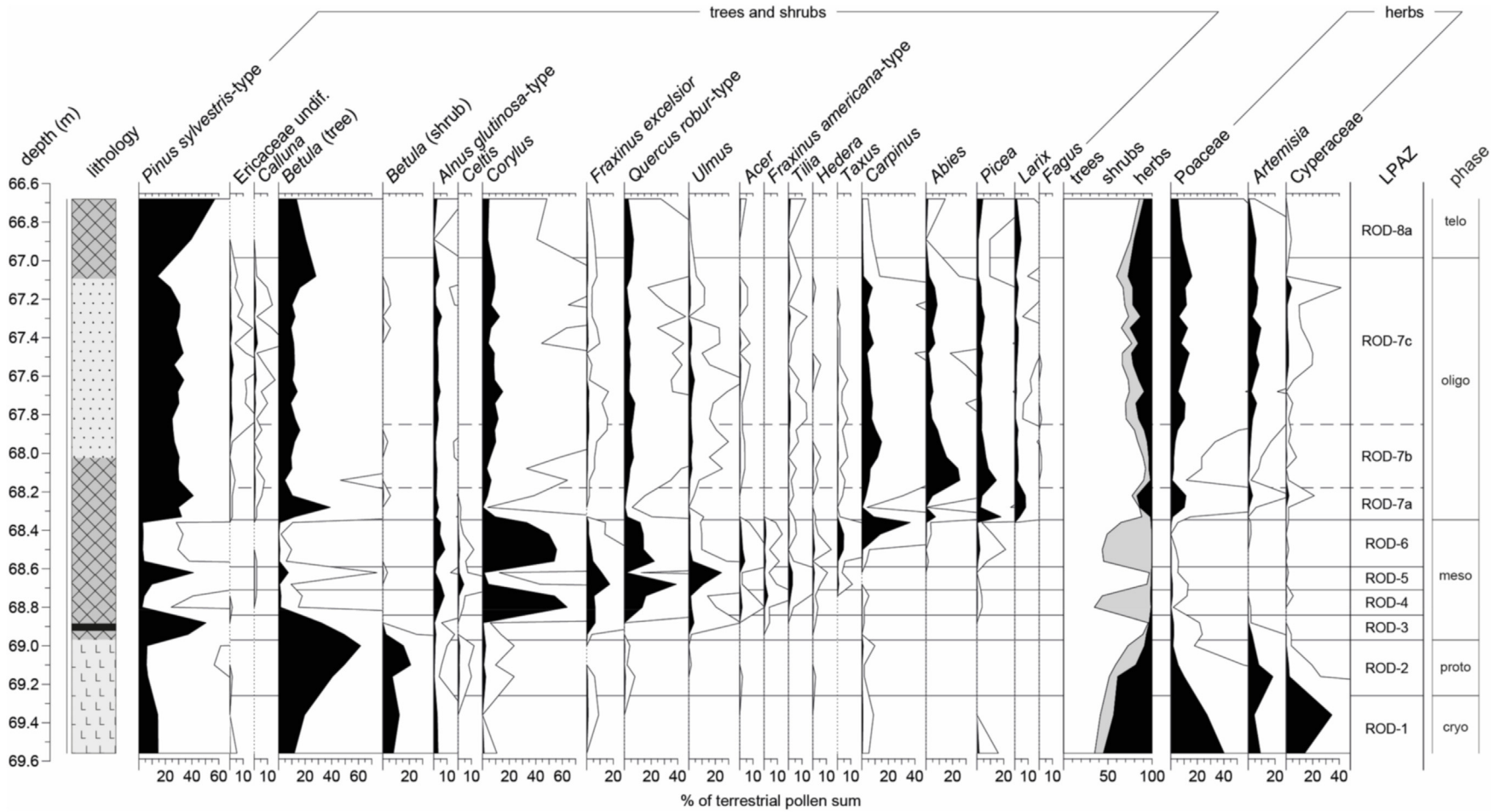

Fig. 6. Pollen percentage diagram (selected taxa) of the proto-, meso-, and oligocratic interglacial (ROD-2 to ROD-7c). Black lines represent 10x exaggeration. Statistically significant local pollen assemblage zones (LPAZ) are delimited with continuous lines, sub-zones are represented by dashed lines (lithological key: see Fig. 4).

setback. Percentages of *Tilia* reach the empirical limit in ROD-4, and *Alnus glutinosa*- as well as *Fraxinus americana*-type show local peaks in percentages and concentrations. Although percentages of *Alnus glutinosa*-type are comparable to ROD-1, its concentrations are steadily increasing since the beginning of the sequence to a peak in ROD-4.

ROD-5 is characterized by AP >95% with a weaker contribution of shrubs. This is due to a massive setback of *Corylus* percentages, which is similarly expressed in the concentrations. Especially percentages and concentrations of *Pinus sylvestris*-type strongly increase but also *Celtis*, *Fraxinus excelsior*-, *Quercus robur*-type, *Ulmus, Tilia*, and *Hedera* reach peaks, substituting *Corylus*.

In ROD-6 total terrestrial pollen concentrations reach maximum values of >2.6 million grains per cm^3. AP stay >95% with a strong contribution of (recovering) *Corylus*, similar to ROD-4. *Quercus robur*-, *Fraxinus excelsior*-, and *Alnus glutinosa*-type are important parts of the pollen assemblage of ROD-6, which is also characterized by the re-appearance of *Picea* pollen and single grains of *Ilex*, *Buxus*, *Sorbus*-type, and *Vitis*. Percentages of *Taxus* pollen reach c. 5% followed by a distinct peak of *Carpinus* (>30%) at the end of the zone. Although tree percentages stay low throughout the zone (50–70%), their concentrations increase to a level similar to ROD-3 and ROD-5 at the end of ROD-6.

Summing up we infer a shift from protocratic *Betula* (ROD-2) to early mesocratic *Pinus sylvestris* dominated nemoboreal forests (ROD-3). This vegetation change was likely driven by further climate warming. Our interpretation is supported by the synchronous initial expansion of temperate trees such as *Ulmus* and *Fraxinus* (in Central Europe most likely *F. excelsior* rather than *F. angustifolia*). Thus, the steadily increasing sample scores along PCA axis 1 (Fig. 4) may reflect warmer climate conditions.

Temperate deciduous forest vegetation dominated by *Corylus* and *Quercus* established during zones ROD-4 and ROD-6. *Taxus*, *Ilex*, *Buxus,* and *Hedera helix* expanded or established first stands, probably in response to a shift towards a warm and oceanic climate, thus indicating full interglacial conditions. This interpretation of peaking interglacial climate forcing is supported by maximum sample scores reached during zones ROD-4 and ROD-6 (Fig. 3). The two periods with abundant *Corylus* are interrupted by a short-lived expansion (ROD-5) of temperate deciduous trees such as *Quercus*, *Fraxinus excelsior*, *Ulmus*, and *Tilia*. The pollen data also suggest that *Pinus sylvestris* re-expanded during this zone. Based on the fact that other boreal species, e.g. *Picea* or *Larix,* did not expand during the same time span, this general trend towards temperate vegetation was probably caused by local disturbances (e.g. fire) and/or an increase in hygric continentality rather than by climate cooling.

3.3.4. Oligocratic (late-temperate) interglacial vegetation (ROD-7; 68.3–67 m)

The percentages of arboreal pollen (AP) decrease to c. 80% in sub-zone ROD-7a, and pollen abundances of temperate species decline (most markedly *Carpinus* and *Quercus robur*-type) while tree *Betula, Pinus sylvestris*-type, and *Larix* peak. Pollen of herbaceous taxa is more important compared to ROD-6, mainly due to Poaceae and *Artemisia*, but also because of Apiaceae and *Filipendula*. In the following sub-zone ROD-7b the percentages of AP rise again to c. 95%, a recovery associated with major peaks of first *Picea* and *Abies* (together with *Abies* stomata) and later *Carpinus*. *Pinus sylvestris*-type, tree *Betula*, and *Larix* are still major components of the assemblage, though less important than in the previous sub-zone ROD-7a. *Fraxinus excelsior*-, *Quercus robur*-type, *Ulmus*, *Acer*, *Taxus*, and *Hedera* re-occur after sub-zone ROD-7a but are less frequent than in ROD-6. For the first time we found single grains of *Fagus* in this sub-zone, while *Celtis* pollen does not occur anymore. The following sub-zone ROD-7c is characterized by a steady decline in AP to c. 75%, mostly at the expenses of *Abies*, *Carpinus*, *Picea*, and *Larix*. Percentages of *Pinus sylvestris*-type and tree *Betula* remain at levels comparable to sub-zone ROD-7b. At the end of ROD-7c, percentages and concentrations of *Quercus robur*-type, Poaceae, and *Artemisia* increase when *Calluna* declines.

Based on these results we infer a transient decline of *Carpinus, Quercus, Abies, Taxus*, and *Picea* during ROD-7a. The expansion of cold-adapted trees (e.g. *Larix, Pinus cembra*) and pioneers (e.g. *Betula*) together with upland herbs points to a marked reorganization of vegetation, which we consider to have been induced by climate cooling. Pollen assemblages in ROD-7b imply that after ROD-7a forests recovered but shifted from temperate deciduous (ROD-6) to nemoboreal forests, dominated by *Abies, Carpinus*, and *Picea* (ROD-7b). *Abies* was locally present at Rodderberg as inferred by the occurrence of single stomata. Boreal trees such *Picea abies, Pinus sylvestris*, and *Betula pendula* might have occupied the Eifel and the Westerwald at higher elevations. Alternatively, the northern limit of boreal forests might have shifted further south and thus closer to the study site. At the end of ROD-7c, boreal *Picea abies* and *Larix*, the heath shrub *Calluna*, moisture-demanding *Salix* as well as temperate *Abies* and *Carpinus* declined, while *Juniperus* and temperate *Quercus* expanded, and the forest opened. This shift was probably linked to reduced moisture availability and/or more continental conditions e.g. promoting late frost to which *Abies* is susceptible (see also steadily declining sample scores on PCA axis 1 from ROD-7b to ROD-7c).

3.3.5. Telocratic (post-temperate) interglacial vegetation (ROD-8; 67–64.8 m)

In sub-zone ROD-8a percentages of arboreal pollen (AP) reach values >90% and those of *Pinus sylvestris*-type together with tree *Betula*, *Corylus*, and *Quercus robur*-type are most abundant. Pollen of *Pinus cembra*-type, *Picea*, *Larix*, and *Alnus glutinosa*-type show continuous abundances throughout ROD-8a. A phase during which percentages of herbaceous taxa increase occurs at c. 66 m. As this phase is represented by just one sample originating from sandy material with a strong decrease in terrestrial pollen concentrations, caution is due when interpreting this pollen signal. ROD-8b is characterized by a major increase in percentages and concentrations of both *Larix* and *Pinus sylvestris*-type. Percentages of temperate tree taxa like *Quercus robur*-type, *Ulmus*, and *Tilia* and boreal tree *Betula* decline. Concentrations of the latter, however, do not show a particular reduction. As in ROD-8a, the level at c. 65.5 m depth represents another phase during which the relative abundance of herbaceous pollen increases (e.g. Poaceae and *Artemisia*). Similar to the previous phase, this level was represented by one sample only, and related inferences have thus to be treated with caution. Nevertheless, because the overall terrestrial pollen concentration in this depth level is similar to the one of the samples below and above, the development likely mirrors true variations in vegetation cover. In ROD-8c AP is >80%, temperate taxa like *Quercus robur*-type, *Tilia*, or *Ulmus,* but most prominently *Abies* and *Carpinus,* show increasing and/or high percentage and concentration values. Very interestingly, single pollen grains of oceanic and temperate *Hedera,* which peaks during the mesocratic phase in ROD-5 and ROD-6, were found. However, much in contrast to the mesocratic phase, shrub *Betula* re-expands in this sub-zone.

These results suggest that nemoboreal forests expanded massively (ROD-8a), and that they were dominated by *Pinus sylvestris* and *Betula*, but also *Picea* and *Larix*. The latter tree developed to a major component of the forest around Rodderberg in ROD-8b, while temperate elements such as *Quercus* and *Ulmus* were reduced, possibly due to low temperatures and/or moisture availability. In ROD-8c a last strong recovery of temperate trees and shrubs such as *Abies, Ulmus, Quercus, Corylus, Tilia, Hedera*, and

Carpinus occurred, likely in response to a rather warm final phase of the interglacial. Subsequently, towards the end of ROD-8c, all temperate species strongly declined, likely in response to climate cooling, converting the nemoboreal forests into boreal forests with important shares of *Pinus, Betula*, and *Larix*.

3.3.6. Glacial and interstadial vegetation (ROD-9 to ROD-11; 64.8–58.9 m)

ROD-9 shows low percentages and concentrations of arboreal pollen (AP ca. 20–50%), to which *Pinus sylvestris*-type, tree *Betula*, and *Larix* contribute most. Percentages of shrub *Betula* reach a local maximum in this zone. Percentages and concentrations of herbaceous pollen increase. Poaceae reaches peak values >50%, while *Artemisia* increases to >10%. *Juniperus* pollen is continuously present yet with low percentages. Only single grains of *Salix*, *Fraxinus excelsior*-, *Quercus robur*-type, *Acer*, *Tilia*, and *Carpinus* are found in this zone, whereas pollen of temperate *Ulmus* and *Abies* is completely absent.

ROD-10 starts with a phase of increased percentages of AP (>70%), mainly due to *Pinus sylvestris*-type and tree *Betula*, and to a minor extent also to *Quercus robur*-type, *Corylus*, *Alnus glutinosa*-type, and *Picea*. All of the above-mentioned types also show increasing concentration values compared to the previous zone. Pollen of the trees *Ulmus*, *Acer*, *Fraxinus excelsior*-type, *Tilia*, *Carpinus*, and *Abies* re-occur more frequently in this first part of ROD-10 compared to the previous extremely open zone ROD-9. The sequence continues with increasing percentages and concentrations of both tree and shrub *Betula*, *Juniperus,* and herbaceous pollen, mostly Poaceae and *Artemisia,* the latter reaches peak values of >20%. Percentages of *Larix* have the highest values in the first half and decrease towards the end of ROD-10. The end of the zone is characterized by increasing percentages (>80%) and concentrations of AP with a main contribution of tree and shrub *Betula* and *Pinus sylvestris*-, but also *Quercus robur*-, *Fraxinus excelsior*-type, and *Ulmus* show high values in the last sample. *Juniperus* pollen is no longer part of the assemblage.

In ROD-11a *Pinus sylvestris*-type pollen is most abundant among the AP that increases massively (>80%), in contrast to the previous zone, in which tree *Betula* was the main component. *Larix*, *Picea*, *Quercus robur*-type pollen, and *Corylus* contribute to a lesser extend to the AP. In ROD-11b the abundance of AP stays below 75%. Pollen of Poaceae contributes most to the percentages of herbaceous pollen, with two intervals at 60.4 and 59.6 m in which a major increase in abundance is observed. However, pollen concentrations of Poaceae do not increase in these depths. Instead, the terrestrial pollen concentrations strongly decrease, pointing to a dilution of the sediment probably in response to increasing erosional input.

During the time period recorded in zone ROD-9, the boreal and temperate forests collapsed almost entirely, only most cold-adapted trees as *Larix* and *Pinus cembra* were not reduced building little stands (AP 20–50%). Likely in response to colder and/or drier climate conditions, the landscape evolved into a species rich, herb dominated steppe tundra with relict patches of boreal *Pinus sylvestris*, *P. cembra,* tree *Betula*, and *Larix*. The local survival of *Larix* is inferred by findings of stomata. At the onset of ROD-10 nemoboreal vegetation recovered to some extent to form forest steppes, which were characterized by the co-occurrence of steppic herbs with boreal trees and only minor shares of continental temperate trees or shrubs (e.g. *Quercus*, *Corylus*). In the course of ROD-10, the landscape further opened up and evolved into steppe vegetation with few patches of boreal forest, mainly *Betula* and *Pinus sylvestris.* Cold- and dry-adapted *Larix* prevailed during this time interval. Towards the end of ROD-10, temperate tree taxa like *Quercus*, *Ulmus*, and *Fraxinus excelsior* recovered to form once gain rather closed (AP >80%) nemoboreal forests that endured during ROD-11a, thus likely pointing to interstadial climatic conditions. During the course of ROD-11b, the nemoboreal forests steadily opened up and in contrast to ROD-10, where *Betula* was the major boreal component, *Pinus sylvestris* dominated during ROD-11b. This shift from *Betula* to *Pinus sylvestris* dominance was likely driven by slightly warmer climate conditions in ROD-11 compared to ROD-10, which is supported by the increased values on the PCA axis 1.

4. Discussion

4.1. Biostratigraphical comparison of the lowermost Rodderberg interglacial (LRI) with Central and Western European pollen profiles

Preliminary assessments (Zolitschka et al., 2014) suggest a depositional age of LRI after MIS 13, but prior to the Eemian (MIS 5e; occurrence of *Celtis* pollen). Our novel and detailed palynological analysis confirms this first assumption, consequently, we focus on similarities and differences with known Central and Western European profiles that fall into the period between MIS 7 and MIS 11. Here, we do not compare the LRI with Southern European records like Ioannina (Tzedakis, 1993, 1994), Tenaghi Philippon (Wijmstra, 1969; Wijmstra and Smit, 1976; van der Wiel and Wijmstra, 1987a, 1987b), Lake Ohrid (Sadori et al., 2016; Donders et al., 2021), Valle di Castiglione (Follieri et al., 1988), or marine sequences from the NW Iberian margin (Desprat et al., 2005, 2006, 2007, 2009; Sanchez Goñi et al., 2018) because of ecological and environmental reasons. Specifically, markedly warmer and often summer-drier conditions in Southern Europe result in divergent successional patterns and forest assemblages compared with Western and Central European archives. For example, interglacials recorded in the marine sequences do not show a telocratic boreal phase (Desprat et al., 2007) like most of the Western and Central European records, including Rodderberg. Additionally, frequent occurrences of Mediterranean taxa such as *Pistacia*, *Quercus ilex-, Q. cerris-, Ostrya*-type, *Olea*, and *Cistus* characterize interglacials and interstadials from Southern Europe (e.g. Follieri et al., 1988; Donders et al., 2021), of which *Pistacia*, *Olea*, and *Cistus* also frequently occur in the marine cores from the NW Iberian margin (e.g. Desprat et al., 2007). On the continent this signal diminishes gradually towards higher latitudes to reach small Mediterranean abundances at Velay (~44°N; Reille et al., 2000) and sporadic single occurrences at Les Échets (~46°N; Beaulieu and Reille, 1984). Most importantly, influences of Southern European vegetation are completely absent further north at Rodderberg (~50°N).

Unfortunately, the linkage of terrestrial pollen archives older than the Eemian with the marine stratigraphy is still not fully established in Western and Central Europe. The following discussion is therefore structured into (i) warm phases pre-dating the Eemian and post-dating the Holsteinian, which are roughly concordant with MIS 7 (see review by Stebich et al., 2020), (ii) the Holsteinian, which corresponds to either MIS 9 or MIS 11 (e.g. Reille et al., 2000; Geyh and Müller, 2005), (iii) the Kärlich (MIS 11; Bittmann, 1992), and (iv) the Rhume/Bilshausen (MIS 11 or MIS 13; Bittmann and Müller, 1996; Kühl and Gobet, 2010) interglacials of the Cromerian Complex.

4.1.1. Warm phases between the Eemian and the Holsteinian interglacials

Several records of warm phases from pre-dating the Eemian and post-dating the Holsteinian are known from Germany (see review by Stebich et al., 2020) and they are roughly concordant with MIS 7. They are characterized as comparably weak warm phases (Lang and Wolff, 2011), which has been globally inferred from e.g. reconstructions of North Atlantic sea surface temperatures (Lawrence et al., 2009), temperatures obtained from Antarctic ice cores (Jouzel

et al., 2007), and global benthic $\delta^{18}O$ signals (Lisiecki and Raymo, 2005). As a likely consequence of such rather cool and variable climatic conditions during MIS 7, many terrestrial archives in Western and Central Europe show comparably small shares of temperate tree and other thermophilous taxa. Falling into this period are e.g. the Leck interstadial (Fig. 1a; Urban et al., 2011) and the Hoogeveen interstadial (Zagwijn, 1973; de Jong, 1988). In other Western and Central European archives, the weak presence or absence of temperate *Taxus* and/or *Abies* conifer forests characterize the vegetational composition during MIS 7, e.g. the three pre-Eemian warm phases of Neualbenreuth Maar (Stebich et al., 2020), Bouchet 1–3 of the long sequence from Velay (Fig. 1a; Reille et al., 2000; Beaulieu et al., 2001), at Schöningen (Urban, 2007) as well as at Wacken (Menke, 1968) and Dömnitz (Erd, 1973) (Fig. 1a). We note, however, that in the case of the latter two archives, the missing *Abies* phase may be explained by a sedimentary hiatus. Nevertheless, also the latter two sequences show a relatively weak abundance of temperate deciduous taxa (e.g. *Quercus*, *Corylus*, *Ulmus*, and *Fraxinus*) compared to *Pinus*, *Betula,* and *Picea* during the warmest phases. In the Reinsdorf sequence (Urban, 1995, 2007) from the Schöningen site (Fig. 1a), this pattern is even more pronounced as temperate deciduous taxa are nearly absent during the warmest phase (LPAZ R 3a) prior to the *Carpinus-Abies* phase (LPAZ R 3 b). Contrarily, the vegetation during the LRI clearly shows full interglacial conditions with a pronounced mesocratic phase comprising closed temperate deciduous forest, a *Taxus* phase, the occurrence of thermophilous evergreen broadleaved *Hedera*, *Buxus*, *Ilex* as well as a well-developed oligocratic phase with *Abies*. Nevertheless, dominating temperate deciduous forest vegetation during the mesocratic phase of Nachtigall 1 (Fig. 1a; Kleinmann et al., 2011) are comparable to the LRI. Importantly, and contrarily to the LRI, *Celtis* and a distinct *Taxus* phase prior to the maximum expansion of *Carpinus* are absent during Nachtigall 1. The same accounts for the second warm phase in the Göttingen/Ottostraβe profile (Fig. 1a; Grüger et al., 1994; Grüger, 1996), which have been suggested to be time equivalents (Kleinmann et al., 2011) but originally placed to the Cromerian Complex (Grüger et al., 1994; Grüger, 1996). A further biostratigraphical comparison of our LRI with Nachtigall 1 is hampered by the fact that the latter sequence is fragmentary and interrupted by two allochthonous units with high amounts of reworked pollen. Additionally, the pollen assemblages are strongly dominated by local fen vegetation (e.g. *Alnus*, *Betula*; Kleinmann et al., 2011).

Most of the post-Holsteinian warm phases from Western and Central Europe do not have occurrences of *Celtis* during the warmest phases, e.g. in France Bouchet 1–3 (Reille et al., 1998) and in Switzerland Meikirch 1–3 (Welten, 1982; Preusser et al., 2005). The same is also the case for records of warm stages in Germany such as Reinsdorf and Schöningen (Urban et al., 1991; Urban, 2007), Wacken (Menke, 1968), Dömnitz (Erd, 1973), Nachtigall (Kleinmann et al., 2011), and Göttingen/Ottostraβe (Fig. 1a). Single grains of *Celtis* were only found in the sediment sequence of Erkner, east of Berlin (Cepek, 1986), during a warm phase, which was attributed to the Dömnitz interglacial. However, the stratigraphic position and the autochthonous deposition of these single grains are debatable (Bittmann, 2012). Another exception is the upper warm phase of Höhenmoos, Southern Germany (Herz et al., 2014), in which small abundances of *Celtis* pollen occur in consecutive samples. In general, the upper warm phase at Höhenmoos is comparable to our LRI. Yet, there are major differences between the two archives, which makes a biostratigraphic correlation difficult. The first one is the different timing of *Larix* occurrences, which is recorded during the protocratic phase together with *Pinus* and *Betula* at Höhenmoos, but is missing during this phase in the LRI, and instead present during the oligocratic phase together with *Abies* and *Carpinus*. Another difference is the timing of the *Ulmus* expansion, which occurs before the *Quercus* and *Fraxinus* expansions at Höhenmoos (Profile IV in Herz et al., 2014; note that *Ulmus* is the first temperate deciduous tree to establish). During the LRI, *Ulmus* only expanded massively (ROD-5) after the initial establishment of a temperate deciduous forest with *Fraxinus excelsior, Quercus*, and *Corylus* (ROD-3 and ROD-4). Taken together, the LRI sequence is characterized by a pronounced interglacial and mesocratic pollen signature, which is lacking in most central European pollen records assigned to MIS 7. Given these discrepancies (climatically rather cool and unstable conditions in central Europe, occurrences of characteristic taxa, and successional patterns), we refrain from correlating the LRI with any of the warm, supposedly interstadial phases, that have been recorded between the Holsteinian and the Eemian.

4.1.2. Holsteinian interglacial (MIS 9 or MIS 11)

The vegetation of the Holsteinian interglacial has been characterized thoroughly on a European scale, and many profiles have been described from Germany (e.g. Erd, 1973; Müller, 1974; Erd et al., 1987; Diehl and Sirocko, 2007; Koutsodendris et al., 2010; Eiβmann et al., 2020). Conventionally, the Holsteinian interglacial has been assigned to MIS 11 (e.g. Sarnthein et al., 1986; Urban, 1995; Reille et al., 2000; Lauer and Weiss, 2018; Tucci et al., 2021), but first U/Th dates of the type section at Bossel, Germany, provided MIS 9 ages (c. 340–325 ka BP; Geyh and Müller, 2005). Typical for Holsteinian-type interglacials are (i) the presence of *Pterocarya* (usually c. 1–2%) during the oligocratic phase together with *Abies*, (ii) early occurrences of *Picea* and *Alnus*, and (iii) a short-lived mid-interglacial climate deterioration after the *Taxus* and the initial *Carpinus* expansion, causing a shift from a closed temperate to more open boreal forest vegetation (Geyh and Müller, 2005; Nitychoruk et al., 2006; Bittmann, 2012). *Celtis* is regularly found in Holsteinian profiles. Early occurrences of *Picea* and *Alnus* as well as the continuous presence of *Celtis* during the mesocratic phase would allow to biostratigraphically correlate the LRI and the Holsteinian. Sub-zone ROD-7a of the LRI potentially corresponds to the mid-interglacial cooling (*Carpinus*-setback) recorded in Holsteinian profiles, e.g. Döttingen (Fig. 7b, zone 4c). However, at Döttingen the expansion of thermophilous taxa (e.g. *Taxus*) as well as the stable abundances of boreal taxa during this phase rather point to drivers other than climate. Similarly, in the Holsteinian profile of Gröbern-Schmerz (Eiβmann et al., 2020), the *Carpinus*-setback comes along with expansions of not only boreal forest, but also of temperate taxa like *Corylus*, *Fraxinus*, and *Abies*. In fact, the vegetational dynamics during sub-zone ROD-7a are quite different from Holsteinian sequences and point towards a severe cooling event with major restructuring of the vegetation towards semi-open boreal forests.

The lack of *Pterocarya* is probably the major difference between the LRI and Holsteinian profiles. A possible explanation could be that *Pterocarya fraxinifolia* is a riparian species (Song et al., 2021) and thus dependent on locally favourable, i.e. wet conditions. In fact, *Pterocarya* abundances and their duration show local variations among Holsteinian sites, from discontinuous occurrences (Kühl and Litt, 2007; Eiβmann et al., 2020) to continuous abundances up to 5% (Diehl and Sirocko, 2007). However, the Döttingen Dry Maar, 460 m a.s.l. (Fig. 1a; Diehl and Sirocko, 2007), the closest Holsteinian profile to Rodderberg and hence the best possible Holsteinian reference despite its higher elevation (313 m difference), has a distinct phase during which *Pterocarya* was present.

4.1.3. Kärlich interglacial (MIS 11)

The Kärlich interglacial has been dated via the intercalated (or basal) Brockentuff to 396 ± 20 ka ($^{40}Ar/^{39}Ar$) and thus to MIS 11 (van den Bogaard et al., 1989). A characteristic similarity between

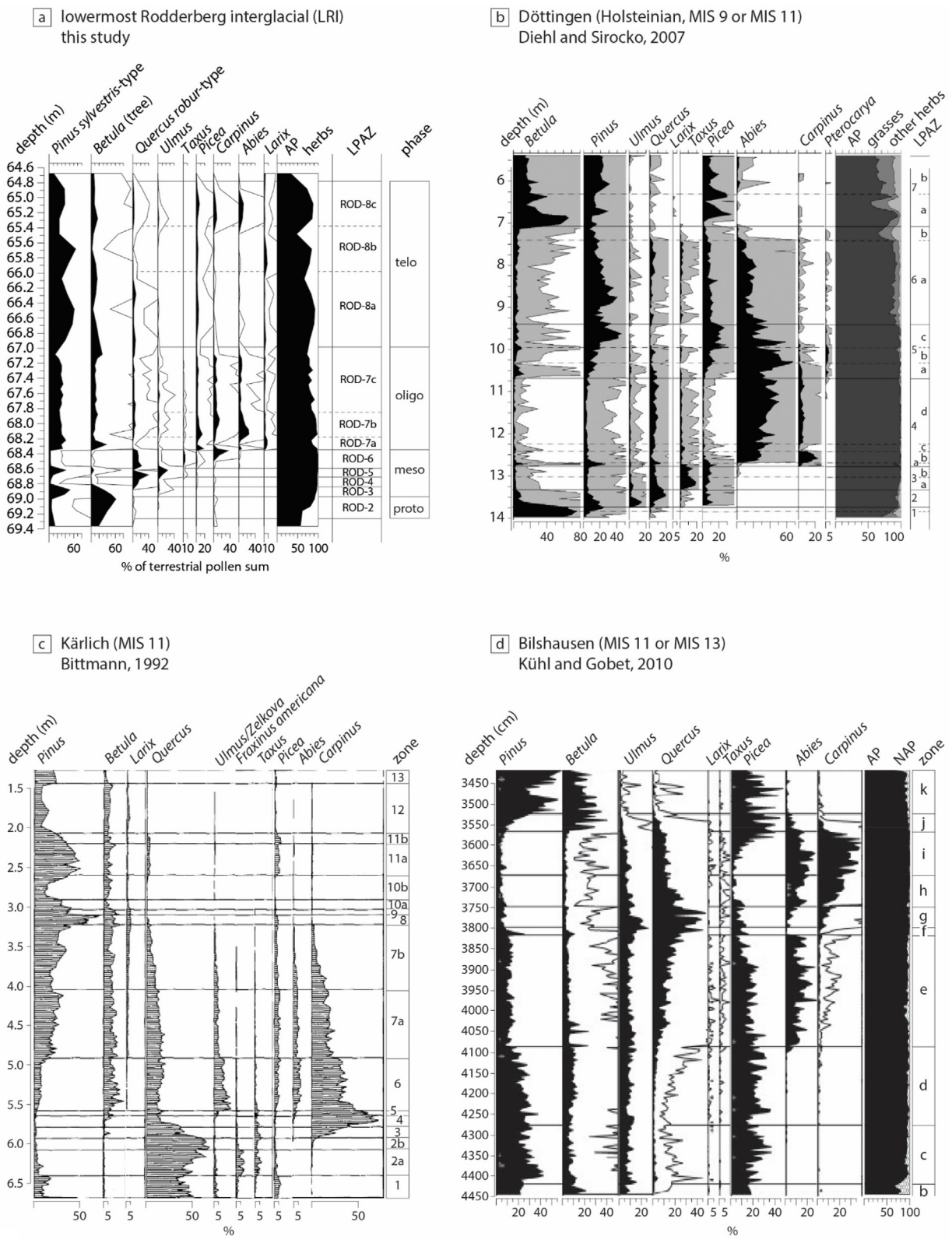

Fig. 7. Pollen percentage diagrams (selected taxa) of the lowermost Rodderberg interglacial (LRI) and its most probable analogues. **a.** Protocratic (proto), mesocratic (meso), oligocratic (oligo) and telocratic (telo) interglacial phases of the LRI. **b.** Holsteinian profile of Döttingen (MIS 9 or MIS 11; modified after Diehl and Sirocko, 2007). **c.** The Kärlich interglacial, dated to 396 ± 20 ka (MIS 11) via $^{40}Ar/^{39}Ar$ (modified after Bittmann, 1992), has been correlated with the second part from the **d.** Bilshausen interglacial (MIS 11 or MIS 13; modified after Kühl and Gobet, 2010).

the LRI and the Kärlich interglacial is the continuous presence of *Larix* starting already during the oligocratic phase together with *Abies* and *Carpinus* (zone 6 in Fig. 7c). This particular feature stands out because *Larix*, as a cold-adapted boreal species (Da Ronch et al., 2016), usually occurs during pre-temperate (Herz et al., 2014) and post-temperate interglacial phases (e.g. Döttingen: Diehl and Sirocko, 2007, Fig. 7b; Reinsdorf: Urban, 2007), or is completely absent (e.g. Gröbern-Schmerz: Eiβmann et al., 2020, Kühl and Litt, 2007; Munster-Breloh: Müller, 1974). The negligible presence of *Pterocarya* (Geyh and Müller, 2007), the presence of *Celtis*, and especially the occurrence of *Fraxinus americana*-type pollen during the mesocratic phase of the Kärlich interglacial are in best agreement with the LRI (Fig. 7c). The tephra layer at the onset of ROD-3 could be further evidence for correlating the LRI with MIS 11. In fact, several eruptions of the Riedener Caldera (East Eifel Volcanic Field) occurred between c. 420 and 400 ka (MIS 11; van den Bogaard, 1995; Schmincke, 2007). Subsequently, the East Eifel Volcanic Field was inactive during the time period between MIS 10 and MIS 7, i.e. until c. 215 ka (Förster and Sirocko, 2016). Additionally, and comparable to the LRI after the telocratic phase (i.e. after ROD-8c; Fig. 4a), a stadial (Mühlheim I; zones 9 and 10 in Fig. 7c) and an interstadial (Kettiger; zone 11 in Fig. 7c) period follow the Kärlich interglacial. However, the short-term vegetational change towards more boreal forests (zone ROD-7a in Fig. 7a) as well as the unstable telocratic phase are both missing in the Kärlich profile. Possible explanations could be that the assemblage change in zone ROD-7a was in fact not driven by climate, but rather reflects landscape modifications due to e.g. landslides, which were colonized by herbaceous vegetation and pioneer trees birch and pine.

4.1.4. Rhume/Bilshausen (MIS 11 or MIS 13)

The younger part of the Bilshausen interglacial (Müller, 1965, 1992; Kühl and Gobet, 2010) has been discussed to be time equivalent to the Kärlich interglacial (Bittmann, 1992; Bittmann and Müller, 1996). Although less likely, an MIS 13 age cannot be totally excluded, since the sequence has never been dated directly (Kühl and Gobet, 2010). During the oligocratic phase of the Bilshausen interglacial, Müller (1965) noticed a short-term (c. 400 years) change from closed temperate forests dominated by *Abies*, *Quercus*, *Ulmus*, and *Picea* to more open nemoboreal forests dominated by *Pinus* and *Betula*. According to the author, this vegetational change was likely driven by climate. In a new profile from Bilshausen, Kühl and Gobet (2010) equally found a *Pinus* and *Betula* expansion, and *Abies* decline during the oligocratic phase (zone f in Fig. 7d). This event could be an analogue of the vegetational changes observed in ROD-7a. However, in contrast to zone ROD-7a of Rodderberg, other temperate trees like *Quercus*, *Ulmus*, and *Tilia* did not decline during this event at Bilshausen, which may suggest other drivers than climate.

Both Bilshausen profiles (Müller, 1965; Kühl and Gobet, 2010) show high variability of pollen data in the telocratic phase (i.e. fluctuating NAP, boreal elements, and re-appearance of temperate taxa) likely resulting from unstable climatic conditions towards the end of the interglacial (zones j and k in Fig. 7d). Although the last recovery of temperate trees in ROD-8c is more prominent compared to observations of the Bilshausen interglacial, the telocratic phase of the LRI is similarly unstable. Additional similarities of the Bilshausen interglacial with the LRI are the early presence of *Larix*, the absence of *Pterocarya*, and the occurrence of *Celtis*. Along with these similarities of the LRI with Bilshausen, certain dissimilarities have to be noted. In fact, a typical (boreal) afforestation phase with *Pinus* and *Betula* is missing at Bilshausen. Instead, afforestation took place with *Pinus*, *Alnus*, *Picea*, and *Ulmus* (Müller, 1965). In contrast to the LRI, *Ulmus* is strongly represented throughout the interglacial. Furthermore, the relative timing of *Carpinus* and *Abies* expansions is inverse at Bilshausen compared to the LRI. The Bilshausen profile suggests the occurrence of a *Tilia* decline corresponding to a c. 4 mm thick tephra layer 5–6 ka after the above-mentioned *Pinus* and *Betula* expansion during the *Abies* phase (Müller, 1992). No such tephra layer has been observed during the LRI or during the Kärlich interglacial, making them more similar, if compared to Bilshausen.

5. Conclusions

We have analysed in more detail the oldest interglacial within the Rodderberg sediment archive, until today only described by four palynological samples. Although reworked pollen is present predominantly at the base of the analysed section, most probably deposited directly after the formation of the maar crater, the general trends in the climate-driven vegetation dynamics reveal a vegetation development which is typical for an interglacial. Based on the vegetation assemblage and succession, our analyses suggest a depositional age prior to MIS 7, which is in accordance with previous studies. The possibility of the LRI to be equivalent to the Holsteinian is still debatable since the lack of *Pterocarya* pollen is only a weak proof of the physical absence of this species. A correlation of the LRI with the Rhume/Bilshausen interglacial is possible. However, the correlation with the Kärlich interglacial, dated to 396 ± 20 ka by $^{40}Ar/^{39}Ar$, is more convincing according to the pollen assemblages and successional patterns (timing of *Larix* expansion, relative timing of *Carpinus* and *Abies*, *Fraxinus americana*-type pollen) as well as the tephra-stratigraphy. This marked biostratigraphic correlation with the $^{40}Ar/^{39}Ar$-dated Kärlich interglacial places the LRI into MIS 11. Ongoing investigations, e.g. new luminescence dating, characterisation of present tephra-layers as well as palynological analyses of the superposed interglacial layers, will hopefully help to solve the still open questions.

Author statement

PS, WT, FS, EG, and BZ conceptualised the study. IH did the lithological analyses and the subsampling for pollen analysis. PS conducted the palynological investigations with support of EG and FB. Moreover, PS analysed the data numerically, visualised the results and wrote the first draft of the manuscript. FS and BZ acquired the funding. All authors contributed to discussions, revised the draft version of the manuscript and agree on the science and the style of the manuscript.

Declaration of competing interest

The authors declare that they have no known competing financial interests or personal relationships that could have appeared to influence the work reported in this paper.

Data availability

Pollen data will be openly accessible via the European Pollen Database.

Acknowledgements

We thank Jacqueline van Leeuwen for her support in pollen determination, Franz Binot for the geological and historical tour in the study area and the participants of the two Rodderberg workshops for lively discussions. The constructive feedback of the reviewers is cordially acknowledged. The coring of ROD11 was funded by the Leibniz Institute for Applied Geophysics Hannover (LIAG). Special thanks are directed to Manfred Schaefer, the owner of

"Broichhof", who supported all drilling activities carried out on his property. Sedimentological analyses were funded by the Deutsche Forschungsgemeinschaft (DFG; project number 420499726) awarded to Bernd Zolitschka. The corresponding author was funded by the Swiss National Science Foundation (SNSF; project number 175555) awarded to Fritz Schlunegger.

References

Aaby, B., Berglund, B.E., 1986. In: Berglund, B.E. (Ed.), Characterisation of Lake and Peat Deposits. Handbook of Holocene Palaeoecology and Palaeohydrology. Wiley, New York, pp. 231–246.

Beaulieu, J.-L. de, Andrieu-Ponel, V., Reille, M., Grüger, E., Tzedakis, P.C., Svobodova, H., 2001. An attempt at correlation between the Velay pollen sequence and the Middle Pleistocene stratigraphy from central Europe. Quat. Sci. Rev. 20 (16–17), 1593–1602. https://doi.org/10.1016/S0277-3791(01)00027-0.

Beaulieu, J.-L. de, Reille, M., 1984. The pollen sequence of Les Échets (France): a new element for the chronology of the upper Pleistocene. Géogr. Phys. Quaternaire 38 (1), 3–9.

Bennett, K.D., 1996. Determination of the number of zones in a biostratigraphical sequence. New Phytol. 132 (1), 155–170. https://doi.org/10.1111/j.1469-8137.1996.tb04521.x.

Beug, H.-J., 2004. Leitfaden der Pollenbestimmung für Mitteleuropa und angrenzende Gebiete. Pfeil, München.

Birks, H.J.B., 1968. The identification of Betula nana pollen. New Phytol. 67 (2), 309–314. https://doi.org/10.1111/j.1469-8137.1968.tb06386.x.

Birks, H.J.B., Gordon, A.D., 1985. Numerical Methods in Quaternary Pollen Analysis. Acad. Press, London.

Birks, H.J.B., Tinner, W., 2016. Past Forests of Europe. In: San-Miguel-Ayanz, J., Rigo, D. de, Caudullo, G., Durrant, T.H., Mauri, A. (Eds.). European atlas of forest tree species. Publication Office of the European Union, Luxembourg, pp. 36–39.

Bittmann, F., 1991. Vegetationsgeschichtliche Untersuchungen an mittel- und jungpleistozänen Ablagerungen des Neuwieder Beckens (Mittelrhein). jrgzm 38 (1), 83–190. https://doi.org/10.11588/jrgzm.1991.1.84016 (83-190 Seiten/Jahrbuch des Römisch-Germanischen Zentralmuseums Mainz, Bd. 38 Nr. 1 (1991.

Bittmann, F., 1992. The Kärlich interglacial, Middle Rhine region, Germany: vegetation history and stratigraphic position. Veg. Hist. Archaeobotany 1, 243–258. https://doi.org/10.1007/bf00189501.

Bittmann, F., 2012. In: Behre, K.-E. (Ed.), Die Schöninger Pollendiagramme und ihre Stellung im mitteleuropäischen Mittelpleistozän. Die chronologische Einordnung der paläolithischen Fundstellen von Schöningen: Band 1. Römisch-Germanisches Zentralmuseum, Mainz.

Bittmann, F., Müller, H., 1996. In: Turner, C. (Ed.), The Kärlich Interglacial Site and its Correlation with the Bilshausen Sequence. The Early Middle Pleistocene in Europe. Balkema, Rotterdam, pp. 187–193.

Cepek, A.G., 1986. Quaternary stratigraphy of the German democratic republic. Quat. Sci. Rev. 5, 359–364. https://doi.org/10.1016/0277-3791(86)90197-6.

Clegg, B.F., Tinner, W., Gavin, D.G., Hu, F.S., 2005. Morphological differentiation of Betula (birch) pollen in northwest North America and its palaeoecological application. Holocene 15 (2), 229–237. https://doi.org/10.1191/0959683605hl788rp.

Da Ronch, F., Caudullo, G., Tinner, W., Rigo, D. de, 2016. In: San-Miguel-Ayanz, J., Rigo, D. de, Caudullo, G., Durrant, T.H., Mauri, A. (Eds.), Larix Decidua and Other Larches in Europe: Distribution, Habitat, Usage and Threats. European atlas of forest tree species. Publication Office of the European Union, Luxembourg.

de Jong, J., 1988. Climatic variability during the past three million years, as indicated by vegetational evolution in northwest Europe and with emphasis on data from The Netherlands. Philos. Trans. R. Soc. Lond. B Biol. Sci. 318 (1191), 603–617.

Desprat, S., Sanchez Goñi, M.F., McManus, J.F., Duprat, J., Cortijo, E., 2009. Millennial-scale climatic variability between 340 000 and 270 000 years ago in SW Europe: evidence from a NW Iberian margin pollen sequence. Clim. Past 5 (1), 53–72. https://doi.org/10.5194/cp-5-53-2009.

Desprat, S., Sanchez Goñi, M.F., Naughton, F., Turon, J.-L., Duprat, J., Malaizé, B., Cortijo, E., Peypouquet, J.-P., 2007. In: Sirocko, F., Claussen, M., Sanchez Goñi, M.F., Litt, T. (Eds.), 25. Climate Variability of the Last Five Isotopic Interglacials: Direct Land-Sea-Ice Correlation from the Multiproxy Analysis of North-Western Iberian Margin Deep-Sea Cores. Developments in Quaternary Sciences: The Climate of Past Interglacials. Elsevier, pp. 375–386.

Desprat, S., Sanchez Goñi, M.F., Turon, J.-L., Duprat, J., Malaizé, B., Peypouquet, J.-P., 2006. Climatic variability of Marine Isotope Stage 7: direct land–sea–ice correlation from a multiproxy analysis of a north-western Iberian margin deep-sea core. Quat. Sci. Rev. 25 (9–10), 1010–1026. https://doi.org/10.1016/j.quascirev.2006.01.001.

Desprat, S., Sanchez Goñi, M.F., Turon, J.-L., McManus, J.F., Loutre, M.-F., Duprat, J., Malaizé, B., Peyron, O., Peypouquet, J.-P., 2005. Is vegetation responsible for glacial inception during periods of muted insolation changes? Quat. Sci. Rev. 24 (12–13), 1361–1374. https://doi.org/10.1016/j.quascirev.2005.01.005.

Diehl, M., Sirocko, F., 2007. In: Sirocko, F., Claussen, M., Sanchez Goñi, M.F., Litt, T. (Eds.), 27. A New Holsteinian Pollen Record from the Dry Maar at Döttingen (Eifel). Developments in Quaternary Sciences: The Climate of Past Interglacials. Elsevier, pp. 397–416.

Dieleman, C., Christl, M., Vockenhuber, C., Gautschi, P., Graf, H.R., Akçar, N., 2022. Age of the most extensive glaciation in the alps. Geosciences 12 (1), 39. https://doi.org/10.3390/geosciences12010039.

Donders, T.H., Panagiotopoulos, K., Koutsodendris, A., Bertini, A., Mercuri, A.M., Masi, A., Combourieu-Nebout, N., Joannin, S., Kouli, K., Kousis, I., Peyron, O., Torri, P., Florenzano, A., Francke, A., Wagner, B., Sadori, L., 2021. 1.36 million years of Mediterranean forest refugium dynamics in response to glacial-interglacial cycle strength. P Natl Acad Sci USA 118 (34), e2026111118. https://doi.org/10.1073/pnas.2026111118.

Eißmann, L., Litt, T., Wansa, S., 2020. In: Ehlers, J., Gibbard, P.L., Kozarski, S., Rose, J. (Eds.), Elsterian and Saalian Deposits in Their Type Area in Central Germany. Glacial Deposits in Northeast Europe. CRC Press, pp. 439–464.

Erd, K., 1973. Vegetationsentwicklung und Biostratigraphie der Dömnitz-Warmzeit (Fuhne/Saale 1) im Profil von Pritzwalk/Prignitz. Abh. Zentr. Geol. Inst. 18, 9–48.

Erd, K., Palme, H., Präger, F., 1987. Holsteininterglaziale Ablagerungen von Rossendorf bei Dresden. Z. Geol. Wiss. 15, 281–295.

Erdelen, M., 1984. Bird communities and vegetation structure: I. Correlations and comparisons of simple and diversity indices. Oecologia 61 (2), 277–284. https://doi.org/10.1007/BF00396773.

Follieri, M., Magri, D., Sadori, L., 1988. 250,000-year pollen record from Valle di Castiglione (Roma). Pollen Spores 30, 329–356.

Förster, M.W., Sirocko, F., 2016. The ELSA tephra stack: volcanic activity in the Eifel during the last 500,000 years. Global Planet. Change 142, 100–107. https://doi.org/10.1016/j.gloplacha.2015.07.012.

Geyh, M.A., 2008. 230Th/U-dating of Intergarcial and Interstadial Fen Peat and Lignite: Potential Limits.

Geyh, M.A., Müller, H., 2005. Numerical 230Th/U dating and a palynological review of the Holsteinian/Hoxnian Interglacial. Quat. Sci. Rev. 24 (16–17), 1861–1872. https://doi.org/10.1016/j.quascirev.2005.01.007.

Geyh, M.A., Müller, H., 2007. 26. Palynological and geochronological study of the Holsteinian/Hoxnian/Landos interglacial. In: Sirocko, F. (Ed.), The Climate of Past Interglacials. Elsevier, Boston, MA, pp. 387–396.

Grüger, E., 1996. Palynostratigraphy of the middle Pleistocene sequence from göttingen, otto-strasse. In: Turner, C. (Ed.), The Early Middle Pleistocene in Europe. Balkema, Rotterdam.

Grüger, E., Jordan, H., Meischner, D., Schlie, P., 1994. Mittelpleistozäne Warmzeiten in Göttingen, Bohrungen Ottostraße und Akazienweg. Geol. J. 134, 167–210.

Herz, M., Knipping, M., Kroemer, E., 2014. Excursion A. The rosenheim basin: würmian and pre-würmian deposits and the Höhenmoos interglacial (MIS 7). In: Kerschner, H., Krainer, K., Spötl, C. (Eds.), From the Foreland to the Central Alps: Field Trips to Selected Sites of Quaternary Research in the Tyrolean and Bavarian Alps. Geozon, Berlin, pp. 6–17.

Houston Durrant, T., Rigo, D. de, Caudullo, G., 2016. Alnus incana in Europe: distribution, habitat, usage and threats. In: San-Miguel-Ayanz, J., Rigo, D. de, Caudullo, G., Durrant, T.H., Mauri, A. (Eds.), European Atlas of Forest Tree Species. Publication Office of the European Union, Luxembourg, p. e01ff87+.

Hytteborn, H., Maslov, A.A., Nazimova, D.I., Rysin, L.P., 2005. Coniferous forests. In: Andersson, F.A. (Ed.), Ecosystems of the World. Elsevier, Amsterdam, pp. 23–99.

Jouzel, J., Masson-Delmotte, V., Cattani, O., Dreyfus, G., Falourd, S., Hoffmann, G., Minster, B., Nouet, J., Barnola, J.M., Chappellaz, J., Fischer, H., Gallet, J.C., Johnsen, S., Leuenberger, M., Loulergue, L., Luethi, D., Oerter, H., Parrenin, F., Raisbeck, G., Raynaud, D., Schilt, A., Schwander, J., Selmo, E., Souchez, R., Spahni, R., Stauffer, B., Steffensen, J.P., Stenni, B., Stocker, T.F., Tison, J.L., Werner, M., Wolff, E.W., 2007. Orbital and millennial Antarctic climate variability over the past 800,000 years. Science 317 (5839), 793–796. https://doi.org/10.1126/science.1141038.

Kershaw, P.A., 1997. A modification of the Troels-Smith system of sediment description and portrayal. Quat. Australasia 15 (2), 63–68. https://aqua.org.au/wp-content/uploads/2013/06/qa_vol-15_no-2_1997.pdf#page=66.

Kleinmann, A., Müller, H., Lepper, J., Waas, D., 2011. Nachtigall: a continental sediment and pollen sequence of the Saalian Complex in NW-Germany and its relationship to the MIS-framework. Quat. Int. 241 (1–2), 97–110. https://doi.org/10.1016/j.quaint.2010.10.005.

Knudsen, M.F., Nørgaard, J., Grischott, R., Kober, F., Egholm, D.L., Hansen, T.M., Jansen, J.D., 2020. New cosmogenic nuclide burial-dating model indicates onset of major glaciations in the Alps during Middle Pleistocene Transition. Earth Planet Sci. Lett. 549, 116491. https://doi.org/10.1016/j.epsl.2020.116491.

Kottek, M., Grieser, J., Beck, C., Rudolf, B., Rubel, F., 2006. World Map of the Köppen-Geiger climate classification updated. metz 15 (3), 259–263. https://doi.org/10.1127/0941-2948/2006/0130.

Koutsodendris, A., Müller, U.C., Pross, J., Brauer, A., Kotthoff, U., Lotter, A.F., 2010. Vegetation dynamics and climate variability during the Holsteinian interglacial based on a pollen record from Dethlingen (northern Germany). Quat. Sci. Rev. 29 (23–24), 3298–3307. https://doi.org/10.1016/j.quascirev.2010.07.024.

Kühl, N., Gobet, E., 2010. Climatic evolution during the middle Pleistocene warm period of bilshausen, Germany, compared to the Holocene. Quat. Sci. Rev. 29 (27–28), 3736–3749.

Kühl, N., Litt, T., 2007. 16. Quantitative time-series reconstructions of holsteinian and Eemian temperatures using botanical data. In: Sirocko, F., Claussen, M., Sanchez Goñi, M.F., Litt, T. (Eds.), Developments in Quaternary Sciences: the Climate of Past Interglacials. Elsevier, pp. 239–254.

Lang, N., Wolff, E.W., 2011. Interglacial and glacial variability from the last 800 ka in marine, ice and terrestrial archives. Clim. Past 7 (2), 361–380.

Lauer, T., Weiss, M., 2018. Timing of the Saalian- and Elsterian glacial cycles and the implications for Middle - Pleistocene hominin presence in central Europe. Sci.

Rep. 8 (1), 5111. https://doi.org/10.1038/s41598-018-23541-w.
Lawrence, K.T., Herbert, T.D., Brown, C.M., Raymo, M.E., Haywood, A.M., 2009. High-amplitude variations in North Atlantic sea surface temperature during the early Pliocene warm period. Paleoceanography 24, PA2218. https://doi.org/10.1029/2008PA001669.
Lisiecki, L.E., Raymo, M.E., 2005. A Pliocene-Pleistocene stack of 57 globally distributed benthic $\delta^{18}O$ records. Paleoceanography 20. https://doi.org/10.1029/2004PA001071.
Litt, T., 2007. Climate, vegetation and mammalian faunas in Europe during middle Pleistocene interglacials (MIS 7, 9, 11). In: Sirocko, F., Claussen, M., Sanchez Goñi, M.F., Litt, T. (Eds.), Developments in Quaternary Sciences: the Climate of Past Interglacials. Elsevier, pp. 351–357.
Menke, B., 1968. Beiträge zur Biostratigraphie des Mittelpleistozäns in Norddeutschland (pollenanalytische Untersuchungen aus Westholstein). Meyniana 18, 35–42. https://pascal-francis.inist.fr/vibad/index.php?action=getrecorddetail&idt=geodebrgm6818025499.
Moore, P.D., Webb, J.A., Collinson, M.E., 1991. Pollen Analysis, second ed. Blackwell Scientific Publications, Oxford.
Müller, H., 1965. Eine pollenanalytische Neubearbeitung des Interglazial-Profils von Bilshausen (Unter-Eichsfeld). Geol. Jahrb. 83, 327–352.
Müller, H., 1974. Pollenanalytische Untersuchungen und Jahresschichtenzählungen an der eemzeitlichen Kieselgur Bispingen/Luhre. Geol. Jahrbuch Reihe 21, 149–169.
Müller, H., 1992. Climate changes during and at the end of the interglacials of the cromerian complex. In: Kukla, G.J., Went, E. (Eds.), Start of a Glacial. Springer, pp. 51–69.
Nitychoruk, J., Bińka, K., Ruppert, H., Schneider, J., 2006. Holsteinian Interglacial=Marine Isotope stage 11? Quat. Sci. Rev. 25 (21–22), 2678–2681. https://doi.org/10.1016/j.quascirev.2006.07.004.
Paulick, H., Ewen, C., Blanchard, H., Zöller, L., 2009. The Middle-Pleistocene (~300 ka) Rodderberg maar-scoria cone volcanic complex (Bonn, Germany): eruptive history, geochemistry, and thermoluminescence dating. Int. J. Earth Sci. 98, 1879–1899. https://doi.org/10.1007/s00531-008-0341-0.
Preusser, F., Drescher-Schneider, R., Fiebig, M., Schlüchter, C., 2005. Re-interpretation of the Meikirch pollen record, Swiss Alpine Foreland, and implications for Middle Pleistocene chronostratigraphy. J. Quat. Sci. 20 (6), 607–620. https://doi.org/10.1002/jqs.930.
Reille, M., 1992. Pollen et spores d'Europe et d'Afrique du nord. Laboratoire de Botanique Historique et Palynologie, Marseille.
Reille, M., Andrieu, V., Beaulieu, J.-L. de, Guenet, P., Goeury, C., 1998. A long pollen record from Lac du Bouchet, Massif Central, France: for the period ca. 325 to 100 ka BP (OIS 9c to OIS 5e). Quat. Sci. Rev. 17 (12), 1107–1123.
Reille, M., Beaulieu, J.-L. de, Svobodova, H., Andrieu-Ponel, V., Goeury, C., 2000. Pollen analytical biostratigraphy of the last five climatic cycles from a long continental sequence from the Velay region (Massif Central, France). J. Quat. Sci. 15 (7), 665–685.
Sadori, L., Koutsodendris, A., Panagiotopoulos, K., Masi, A., Bertini, A., Combourieu-Nebout, N., Francke, A., Kouli, K., Joannin, S., Mercuri, A.M., Peyron, O., Torri, P., Wagner, B., Zanchetta, G., Sinopoli, G., Donders, T.H., 2016. Pollen-based paleoenvironmental and paleoclimatic change at Lake Ohrid (south-eastern Europe) during the past 500 ka. Biogeosciences 13 (5), 1423–1437. https://doi.org/10.5194/bg-13-1423-2016.
Sanchez Goñi, M.F., Desprat, S., Fletcher, W.J., Morales-Molino, C., Naughton, F., Oliveira, D., Urrego, D.H., Zorzi, C., 2018. Pollen from the deep-sea: a breakthrough in the mystery of the ice ages. Front. Plant Sci. 9, 38. https://doi.org/10.3389/fpls.2018.00038.
Sarnthein, M., Stremme, H.E., Mangini, A., 1986. The holstein interglaciation: time-stratigraphic position and correlation to stable-isotope stratigraphy of deep-sea sediments. Quat. Res. 26 (3), 283–298. https://doi.org/10.1016/0033-5894(86)90090-6.
Schläfli, P., Gobet, E., van Leeuwen, J.F., Vescovi, E., Schwenk, M.A., Bandou, D., Douillet, G.A., Schlunegger, F., Tinner, W., 2021. Palynological investigations reveal Eemian interglacial vegetation dynamics at Spiezberg, Bernese Alps, Switzerland. Quat. Sci. Rev. 263, 106975. https://doi.org/10.1016/j.quascirev.2021.106975.
Schmidt, E.D., Frechen, M., Murray, A.S., Tsukamoto, S., Bittmann, F., 2011a. Luminescence chronology of the loess record from the Tönchesberg section: a comparison of using quartz and feldspar as dosimeter to extend the age range beyond the Eemian. Quat. Int. 234 (1–2), 10–22. https://doi.org/10.1016/j.quaint.2010.07.012.
Schmidt, E.D., Murray, A.S., Sirocko, F., Tsukamoto, S., Frechen, M., 2011b. IRSL signals from maar lake sediments stimulated at various temperatures. E&G Quat Sci J 60 (1), 105–115. https://doi.org/10.3285/eg.60.1.07.
Schmiedel, I., Goedecke, F., Bergmeier, E., 2019. Plant communities of the Eifel national Park (Germany) – an assessment based on the first permanent plot inventory. Tuexenia 39, 41–74. https://doi.org/10.14471/2019.39.015.
Schmincke, H.-U., 2007. The quaternary volcanic fields of the East and west Eifel (Germany). In: Ritter, J.R.R., Christensen, U.R. (Eds.), Mantle Plumes: A Multidisciplinary Approach. Springer, Berlin, New York, pp. 241–322.
Schwenk, M.A., Schläfli, P., Bandou, D., Gribenski, N., Douillet, G.A., Schlunegger, F., 2022. From glacial erosion to basin overfill: a 240 m-thick overdeepening–fill sequence in Bern, Switzerland. Sci. Drill. 30, 17–42. https://doi.org/10.5194/sd-30-17-2022.
Song, Y.-G., Walas, Ł., Pietras, M., Sâm, H.V., Yousefzadeh, H., Ok, T., Farzaliyev, V., Worobiec, G., Worobiec, E., Stachowicz-Rybka, R., Boratyński, A., Boratyńska, K., Kozlowski, G., Jasińska, A.K., 2021. Past, present and future suitable areas for the relict tree Pterocarya fraxinifolia (Juglandaceae): integrating fossil records, niche modeling, and phylogeography for conservation. Eur. J. For. Res. 140 (6), 1323–1339. https://doi.org/10.1007/s10342-021-01397-6.
Stebich, M., Höfer, D., Mingram, J., Nowaczyk, N.R., Rohrmüller, J., Mrlina, J., Kämpf, H., 2020. A contribution towards the palynostratigraphical classification of the middle Pleistocene in central Europe: the pollen record of the Neualbenreuth maar, northeastern bavaria (Germany). Quat. Sci. Rev. 250, 106681. https://doi.org/10.1016/j.quascirev.2020.106681.
Stockmarr, J., 1971. Tablets with spores used in absolute pollen analysis. Pollen et spores 13 615–621.
ter Braak, C.J.F., Šmilauer, P., 2018. Canoco Reference Manual and User's Guide: Software for Ordination (Version 5.10). Biometris, Wageningen.
Troels-Smith, J., 1955. Characterisation of unconsolidated sediments. Danm. geol. Unders. 3 (10).
Tucci, M., Krahn, K.J., Richter, D., van Kolfschoten, T., Álvarez, B.R., Verheijen, I., Serangeli, J., Lehmann, J., Degering, D., Schwalb, A., Urban, B., 2021. Evidence for the age and timing of environmental change associated with a Lower Palaeolithic site within the Middle Pleistocene Reinsdorf sequence of the Schöningen coal mine, Germany. Palaeogeogr. Palaeoclimatol. Palaeoecol. 569, 110309. https://doi.org/10.1016/j.palaeo.2021.110309.
Tzedakis, P.C., 1993. Long-term tree populations in northwest Greece through multiple Quaternary climatic cycles. Nature 364 (6436), 437–440. https://doi.org/10.1038/364437a0.
Tzedakis, P.C., 1994. Vegetation change through glacial—interglacial cycles: a long pollen sequence perspective. Phios T R Soc B 345 (1314), 403–432. https://doi.org/10.1098/rstb.1994.0118.
Urban, B.…, , 1995. Palynological evidence of younger Middle Pleistocene interglacials (Holsteinian, Reinsdorf and Schöningen) in the Schöningen open cast lignite mine. Meded. Rijks Geol. Dienst 5, 175–186.
Urban, B., 2007. Interglacial pollen records from schöningen, north Germany. In: Sirocko, F., Claussen, M., Sanchez Goñi, M.F., Litt, T. (Eds.), Developments in Quaternary Sciences: the Climate of Past Interglacials. Elsevier, pp. 417–444.
Urban, B., Elsner, H., Hölzer, A., Mania, D., Albrecht, B., 1991. Eine eem- und frühweichselzeitliche Abfolge im Tagebau Schöningen, Landkreis Helmstedt. E&G Quat Sci J 41 (1), 85–99. https://doi.org/10.3285/eg.41.1.07.
Urban, B., Sierralta, M., Frechen, M., 2011. New evidence for vegetation development and timing of Upper Middle Pleistocene interglacials in Northern Germany and tentative correlations. Quat. Int. 241 (1–2), 125–142. https://doi.org/10.1016/j.quaint.2011.02.034.
van den Bogaard, C., van den Bogaard, P., Schmincke, H.-U., 1989. Quartärgeologisch-tephrostratigraphische Neuaufnahme und Interpretation des Pleistozänprofils Kärlich. E&G Quat Sci J 39 (1), 62–86. https://doi.org/10.3285/eg.39.1.08.
van den Bogaard, P., 1995. Quaternary Volcanism: Field Guide Excursion A18. XIV International Congress, Berlin.
van der Wiel, A.M., Wijmstra, T.A., 1987a. Palynology of the 112.8–197.8 m interval of the core Tenaghi Philippon III, middle Pleistocene of Macedonia. Rev. Palaeobot. Palynol. 52 (2–3), 89–117. https://doi.org/10.1016/0034-6667(87)90048-0.
van der Wiel, A.M., Wijmstra, T.A., 1987b. Palynology of the lower part (78–120 M) of the core Tenaghi Philippon II, middle Pleistocene of Macedonia, Greece. Rev. Palaeobot. Palynol. 52 (2–3), 73–88. https://doi.org/10.1016/0034-6667(87)90047-9.
Welten, M., 1982. Pollenanalytische Untersuchungen im Jüngeren Quartär des nördlichen Alpenvorlandes der Schweiz. Beiträge zur geologischen Karte der Schweiz. Stämpfli + Cie AG, Bern.
Wijmstra, T.A., 1969. Palynology of the first 30 metres of a 120 m deep section in Northern Greece. Acta Bot. Neerl. 18 (4), 511–527.
Wijmstra, T.A., Smit, A., 1976. Palynology of the middle part (30-78 metres) of the 120 m deep section in Northern Greece (Macedonia). Acta Bot. Neerl. (25), 297–312.
Williams, J.W., Ordonez, A., Svenning, J.-C., 2021. A unifying framework for studying and managing climate-driven rates of ecological change. Nat Ecol Evol 5 (1), 17–26. https://doi.org/10.1038/s41559-020-01344-5.
Zagwijn, W.H., 1973. Pollenanalytic studies of Holsteinian and Saalian beds in the northern Netherlands. Mededel. Rijks Geol. Dienst 24, 139–156.
Zolitschka, B., Rolf, C., Bittmann, F., Binot, F., Frechen, M., Wonik, T., Froitzheim, N., Ohlendorf, C., 2014. Pleistocene climatic and environmental variations inferred from a terrestrial sediment record–the Rodderberg Volcanic Complex near Bonn, Germany. Z. Dtsch. Ges. Geowiss. 165 (3), 407–424.
Zöller, L., Blanchard, H., 2009. The partial heat – longest plateau technique: testing TL dating of Middle and Upper Quaternary volcanic eruptions in the Eifel Area, Germany. E&G Quat Sci J 58 (1), 86–106.
Zöller, L., Hambach, U., Blanchard, H., Fischer, S., Köhne, S., Stritzke, R., 2011. Der Rodderberg-Krater bei Bonn: ein komplexes Geoarchiv. E&G Quat Sci J 59 (1/2), 44–58. https://doi.org/10.3285/eg.59.1-2.04.